Ultimate strength of high yield strength constructional-alloy circular columns: effect of thermal residual stresses

Autor(en): **Nitta, Akira / Thürlimann, Bruno**

Objekttyp: **Article**

Zeitschrift: **IABSE publications = Mémoires AIPC = IVBH Abhandlungen**

Band (Jahr): **22 (1962)**

PDF erstellt am: **30.04.2024**

Persistenter Link: https://doi.org/10.5169/seals-18810

Ultimate Strength of High Yield Strength Constructional-Alloy Circular Columns — Effect of Thermal Residual Stresses

Résistance limite des barres comprimées à section circulaire, en alliage à haute limite élastique — Influence des contraintes résiduelles thermiques

Tragfähigkeit von Säulen mit Kreisquerschnitt aus legiertem Baustahl mit hoher Fließgrenze — Einfluß von thermischen Eigenspannungen

AKIRA NITTA
National Aeronautical Laboratory, Tokyo *)

BRUNO THÜRLIMANN
Swiss Federal Institute of Technology, Zurich *)

I. Introduction

It is a well-known fact that for columns of intermediate slenderness the use of a high-yield-strength alloy steel will increase the resistance against instability because of its high yield strength which primarily governs the load-carrying capacity of column members in the inelastic range. In structures such as tall built-up towers constructional alloy steel round bars have been frequently used for the tower legs. It should be pointed out, however, that the process of heat treatment for such a material may cause cooling residual stresses and initial out-of-straightness, both of which are significant factors influencing the ultimate strength of columns.

Even though a number of experimental results have been published [1][1]) comparatively little significant work has been done to predict theoretically the thermal residual stresses in circular cylinders. Recently, WEINER and HUDDLESTON [2] showed a solution of the phase-transformation stresses from the standpoint of the flow theory of plasticity. Since the process for obtaining a general solution is very involved it seems almost inevitable to introduce simplifying assumptions when performing numerical calculations. Hence certain constant values of the material properties are used as a common value

---

*) Formerly Fritz Engineering Laboratory Lehigh University, Bethlehem, Pa.

[1]) The numbers in parentheses refer to the list of references. They are listed in order of their occurrence.

for the whole stage of cooling instead of taking the true values corresponding to the variable temperatures.

By including the effect of the residual stresses in steel columns a reasonable approach to the solution of the buckling load was suggested by OSGOOD [3], YANG and others [4]. Extensive studies on rolled wide-flange steel columns have been performed by several investigators [5], [6].

On the other hand, it has been shown that centrally loaded columns can be expected to carry higher loads than that given by the tangent modulus theory [7]. Unfortunately, however, this post-buckling behavior of inelastic columns has never been solved in a general way. FUJITA [8] solved graphically the ultimate strength of H-shape built-up columns including the effect of residual stresses due to welding. The maximum load-carrying capacity of a wide-flange beam-column subjected to an axial thrust and end moments was obtained by GALAMBOS and KETTER [9]. Since these particular solutions are not applicable to any other cross sectional shapes in which the magnitude and the distribution pattern of residual stresses are different, further studies are necessary in order to visualize the true column behavior until failure occurs.

II. Thermal Residual Stresses in Solid Circular Columns

When structural steel members are subjected to quenching operations, two different types of stresses, namely thermal and transformation stresses, will be produced. If the strains arising during the cooling period exceed the elastic limit of the steel at any instance, residual stresses will remain after complete cooling. In general, the formation of such residual stresses is mainly influenced by the initial temperature, the cooling method and the shape and size of the specimen. For those sections which are rapidly cooled by water quenching without subsequent tempering or other stress relieving, the thermal residual stresses become of great importance.

1. General Description of the Analysis

a) Temperature Distribution

When a long circular steel cylinder (radius = R) of initial uniform temperature T_0 is submerged in water, the temperature distribution at co-ordinate r, and time t, can be obtained by making the following assumptions [10]:

1. Cooling takes place polar-symmetrically.
2. There is no variation in temperature along the length of the cylinder.
3. The thermal diffusivity, κ, is independent of temperature.
4. Newton's cooling law holds.

The temperature distribution is as follows:

$$\frac{T(\rho,\tau)}{T_0} = 2c\sum_{i=1}^{\infty}\frac{J_0(m_i\rho)}{(\kappa^2+m_i^2)J_0(m_i)}\exp(-m_i^2\tau), \tag{1}$$

where

$\rho \equiv \frac{r}{R}$ = non-dimensional co-ordinate,

$\tau \equiv \frac{\kappa t}{R^2}$ = non-dimensional time parameter,

c = constant depending upon the initial temperature and radius of the cylinder, and m_i's are parameters that satisfy the equations;

$$m_{i\,1}J(m_i) = cJ_0(m_i), \quad (i=1,2,3\ldots) \tag{2}$$

J_0 and J_1 being Bessel function of order zero and one, respectively.

b) Stress-Strain Relationship at Elevated Temperatures

During the period of cooling from an initial temperature, T_0, to the room temperature (taken as zero degrees), the material is assumed to be isotropic but non-homogeneous due to the variation of temperature in the cross section of the cylinder. For USS "T-1" constructional alloy steel[2]), which was used in the experimental investigation described herein, stress-strain diagrams at various elevated temperatures obtained from simple tension tests[3]) are shown in Fig. 1. In order to simplify the analysis it is assumed that below the yield point, which is determined by the "ordinary 0.2% offset method" on each diagram, the steel behaves as an elastic material with a temperature-dependent modulus of elasticity, $E(T)$. At the level of the yield stress it is assumed that plastic flow takes place without strain-hardening. Hence, an idealized elastic-plastic stress-strain relationship is used for the material at each temperature as shown in the same figure.

Taking any arbitrary time interval $\Delta\tau$ during the cooling stage, the corresponding decrement in temperature $\Delta T(\rho)$ can be obtained from Eq. (1). For the elastic part in the cross section the relationship between the corresponding change of stress $\Delta\sigma$ and of strain $\Delta\epsilon$ will be expressed in the following

---

[2]) USS "T-1" constructional alloy steel is a quenched and tempered steel that, in normal production, is air cooled from the tempering temperature. As part of this investigation, however, the effect of two other possible final heat treatments, stress-relieving after tempering and quenching after tempering, on column strength was studied. "T-1" steel bars for critical applications, such as television towers, are normally cold straightened and stress relieved after air cooling but the effect of this process is covered in a second study.

[3]) This test data were supplied by the United States Steel Corporation.

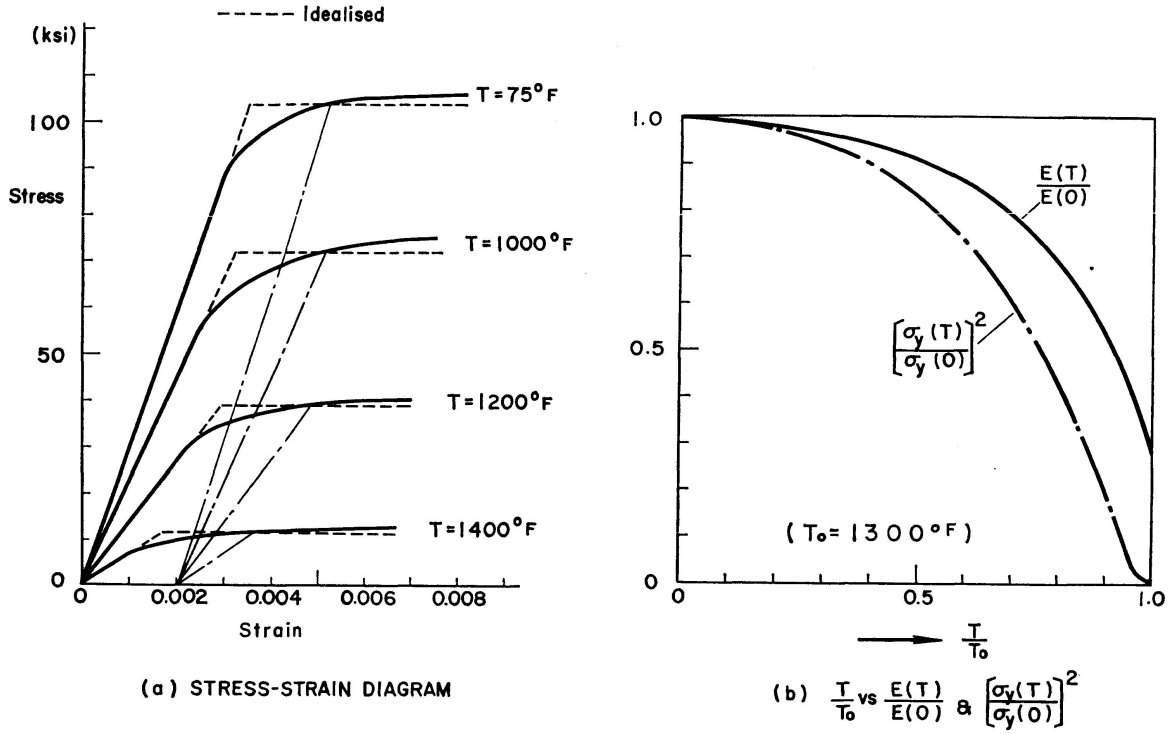

Fig. 1a), b). Stress-strain relationship at various temperatures.

way[4]) (compressive stress and strain being taken as positive):

$$\Delta\epsilon_r = \alpha(T)\Delta T + \frac{1}{E(T)}[\Delta\sigma_r - \nu(T)\{\Delta\sigma_\theta + \Delta\sigma_z\}],$$

$$\Delta\epsilon_\theta = \alpha(T)\Delta T + \frac{1}{E(T)}[\Delta\sigma_\theta - \nu(T)\{\Delta\sigma_z + \Delta\sigma_r\}], \tag{3}$$

$$\Delta\epsilon_z = \alpha(T)\Delta T + \frac{1}{E(T)}[\Delta\sigma_z - \nu(T)\{\Delta\sigma_r + \Delta\sigma_\theta\}],$$

where $\alpha(T)$ is a linear thermal expansion coefficient and $\nu(T)$ is Poisson's ratio.

c) Thermal Stresses

The thermal stresses produced as cooling occurs during the time interval $\Delta\tau$ will be obtained in the following way:

First, if the cylinder is fully restrained at both ends, axial displacements along the length will vanish; thereby

$$\Delta\epsilon_z = 0. \tag{4}$$

---

[4]) Conventional subscripts r, θ and z denote radial, tangential and axial components of the stress and the strain, respectively.

The following equilibrium condition must be satisfied for any element in the cross section.

$$\frac{d(\Delta\sigma_r)}{dr}+\frac{(\Delta\sigma_r)-(\Delta\sigma_\theta)}{r}=0. \tag{5}$$

By letting the corresponding change of radial displacement be Δv, radial and tangential components of strain are given by

$$\Delta\epsilon_r=\frac{d(\Delta v)}{dr},\qquad \Delta\epsilon_\theta=\frac{\Delta v}{r}. \tag{6}$$

From Eqs. (3), (4), (5) and (6), the following differential equation can be obtained:

$$B_1\left[\frac{d^2\omega}{d\rho^2}+\frac{1}{\rho}\frac{d\omega}{d\rho}-\frac{\omega}{\rho^2}\right]+\frac{dB_1}{d\rho}\frac{d\omega}{d\rho}+\frac{dB_2}{d\rho}\frac{\omega}{\rho}=\frac{dB_3}{d\rho}, \tag{7}$$

where

$$\omega\equiv\frac{\Delta v}{R},\qquad \rho\equiv\frac{r}{R},$$

$$B_1\equiv\frac{[1-\nu(T)]}{[1+\nu(T)][1-2\nu(T)]}E(T),$$

$$B_2\equiv\frac{\nu(T)}{[1+\nu(T)][1-2\nu(T)]}E(T),$$

$$B_3\equiv\frac{1}{[1-2\nu(T)]}\alpha(T)\Delta T E(T).$$

When ν, E and α are independent of temperature, both $\frac{dB_1}{d\rho}$ and $\frac{dB_2}{d\rho}$ vanish and Eq. (7) coincides with the known equation [11]:

$$\frac{d^2\omega}{d\rho^2}+\frac{1}{\rho}\frac{d\omega}{d\rho}-\frac{\omega}{\rho^2}=\alpha\frac{1+\nu}{1-\nu}\frac{d(\Delta T)}{d\rho}.$$

The boundary conditions are given as follows:

$$\begin{aligned}&\text{at}\quad \rho=0\qquad \omega=0,\\ &\text{at}\quad \rho=1\quad \Delta\sigma_r=0\end{aligned} \tag{8}$$

which leads to

$$\left[\frac{d\omega}{d\rho}\right]_{\rho=1}+\left[\frac{\nu(T)}{1-\nu(T)}\omega\right]_{\rho=1}=\left[\frac{1+\nu(T)}{1-\nu(T)}\alpha(T)\Delta T\right]_{\rho=1}. \tag{9}$$

The differential Eq. (7) with variable coefficients together with the given boundary conditions Eqs. (8) and (9) can be approximately solved by using the finite difference method. When ν and α are independent of temperature [5]),

---

[5]) See Section d) in this article.

for example, the following N simultaneous equations for N unknowns, ω_i's ($i=1,2,\ldots N$) have been derived as follows:

$$\omega_{i-1}\left[2i-1-\frac{i}{2}(C_i^{i+1}-C_i^{i-1})\right]+\omega_i\left[-4i-\frac{2}{i}+\frac{\nu}{1-\nu}(C_i^{i+1}-C_i^{i-1})\right]$$
$$+\omega_{i+1}\left[2i+1+\frac{i}{2}(C_i^{i+1}-C_i^{i-1})\right]=\alpha\frac{1+\nu}{1-\nu}\frac{i}{N}[C_i^{i+1}\Delta T_{i+1}-C_i^{i-1}\Delta T_{i-1}],$$
$$\text{for } i=1,2,\ldots(N-1)$$
$$\text{with} \qquad \omega_0=0, \tag{10}$$
$$\text{and} \qquad \omega_{N-1}[4N]+\omega_N\left[-4N+4-\frac{1}{1-\nu}\left(\frac{2}{N}+4\right)\right]=$$
$$\alpha\frac{1+\nu}{1-\nu}\left[C_N^{N+1}\Delta T_{N+1}-\left(4+\frac{2}{N}-C_N^{N-1}+C_N^{N+1}\right)\Delta T_N-C_N^{N-1}\Delta T_{N-1}\right],$$

where the subscript i of ω and ΔT denotes the values for $\rho_i=\frac{i}{N}$, and $C_i^{i+1}\equiv\frac{E(\rho_{i+1})}{E(\rho_i)}$, etc.

Since the first and the last equations contain only two unknowns and the rest of them involve three unknowns each, the solution can be easily obtained by successive elimination of the unknowns.

From Eqs. (3), (4) and (6), the incremental axial stress produced in the fixed-end cylinder is given by the following formula:

$$\Delta\sigma_z'=\frac{E(T)}{(1+\nu)(1-2\nu)}\left[\nu\frac{d\omega}{d\rho}+\nu\frac{\omega}{\rho}-(1+\nu)\alpha\Delta T\right]. \tag{11}$$

However, the actual cylinder is free from the resultant force in the axial direction; therefore the following correction term

$$-\frac{1}{A}\int\Delta\sigma_z'dA\,(=-2\int_0^1\Delta\sigma_z'\rho\,d\rho)$$

should be added to the axial stress given by Eq. (11). Thus, finally, the incremental stresses caused by cooling during $\Delta\tau$ will be obtained by the following formulæ:

$$\Delta\sigma_r=\frac{E(T)}{(1+\nu)(1-2\nu)}\left[(1-\nu)\frac{d\omega}{d\rho}+\nu\frac{\omega}{\rho}-(1+\nu)\alpha\Delta T\right],$$
$$\Delta\sigma_\theta=\frac{E(T)}{(1+\nu)(1-2\nu)}\left[\nu\frac{d\omega}{d\rho}+(1-\nu)\frac{\omega}{\rho}-(1+\nu)\alpha\Delta T\right], \tag{12}$$
$$\Delta\sigma_z=\Delta\sigma_z'-2\int_0^1\Delta\sigma_z'\rho\,d\rho.$$

1. Fully elastic case

Transient stresses at any instance of cooling will be obtained as the summations of the incremental stresses computed by Eq. (12), provided that the

material remains within the elastic limit. The latter depends upon the temperature at each location in question.

$$\sigma_{r,\theta,z} = \sum_{\tau=0}^{\tau=\tau} \Delta\sigma_{r,\theta,z}. \tag{13}$$

2. Elastic-plastic case

Applying Mises' condition as the criterion of yielding at various temperatures, the material will remain elastic if

$$J_2 < \tfrac{1}{3}\sigma_y^2(T), \tag{14}$$

where

$$J_2 = \tfrac{1}{6}[(\sigma_r-\sigma_\theta)^2+(\sigma_\theta-\sigma_z)^2+(\sigma_z-\sigma_r)^2]. \tag{15}$$

However, when the value of $J_2(T)$, which is computed by using the stress components based upon Eq. (13), exceeds the value of $\frac{1}{3}\sigma_y^2(T)$, yielding takes place in such regions and a correction for the stresses must be made to get the actual stress distribution. It is assumed that during a time interval $\Delta\tau$, the increment of each stress component $(\Delta\sigma_r)_p$, $(\Delta\sigma_\theta)_p$ and $(\Delta\sigma_z)_p$ in the plastic range is proportional to that of the elastically computed stress component of Eq. (12)[6]), namely,

$$\frac{(\Delta\sigma_r)_p}{\Delta\sigma_r} = \frac{(\Delta\sigma_\theta)_p}{\Delta\sigma_\theta} = \frac{(\Delta\sigma_z)_p}{\Delta\sigma_z} = e.$$

These incremental stresses, $(\Delta\sigma_r)_p$, $(\Delta\sigma_\theta)_p$ and $(\Delta\sigma_z)_p$ thus assumed, satisfy the boundary condition and the equilibrium condition of a small element, because $\Delta\sigma_r$, $\Delta\sigma_\theta$ and $\Delta\sigma_z$ fulfill all these requirements. Then, in the plastic region, the transient stress components at $\tau=\tau_2$ can be expressed in terms of the values at the preceding step, $\tau=\tau_1(\tau_2-\tau_1=\Delta\tau)$ and the plastic stress increments:

$$\sigma_{r,\theta,z}(\tau=\tau_2) = \sigma_{r,\theta,z}(\tau=\tau_1)+e\,\Delta\sigma_{r,\theta,z}. \tag{16}$$

Since in the plastic region, when $\tau=\tau_2$ the yield condition must be satisfied,

$$J_2(\tau=\tau_2) = \tfrac{1}{3}\sigma_y^2(\tau=\tau_2)$$

the following relationship is obtained from Eqs. (15) and (16).

$$\Delta J_2 e^2 + 2\bar{J}_2(\tau_1,\Delta)e + J_2(\tau=\tau_1) - \tfrac{1}{3}\sigma_y^2(\tau=\tau_2) = 0, \tag{17}$$

where

$$\Delta J_2 = \tfrac{1}{6}[(\Delta\sigma_r-\Delta\sigma_\theta)^2+(\Delta\sigma_\theta-\Delta\sigma_z)^2+(\Delta\sigma_z-\Delta\sigma_r)^2],$$

$$\bar{J}_2(\tau_1,\Delta) = \tfrac{1}{6}[(\sigma_r-\sigma_\theta)_{\tau=\tau_1}(\Delta\sigma_r-\Delta\sigma_\theta) + (\sigma_\theta-\sigma_z)_{\tau=\tau_1}(\Delta\sigma_\theta-\Delta\sigma_z)+(\sigma_z-\sigma_r)_{\tau=\tau_1}(\Delta\sigma_z-\Delta\sigma_r)].$$

---

[6]) See Appendix for justification of assumption.

Hence the proportionality factor, e, is given as follows:

$$e = \frac{-\bar{J}_2(\tau_1, \Delta) + \sqrt{\{\bar{J}_2(\tau_1, \Delta)\}^2 + \Delta J_2 \{\frac{1}{3}\sigma_y^2(\tau = \tau_2) - J_2(\tau = \tau_1)\}}}{\Delta J_2}. \tag{18}$$

As a result of this correction for the incremental stresses in the plastic range it becomes necessary to redistribute the stresses in the elastic range so as to maintain the equilibrium of the whole body. For the convenience of the discussion, the incremental correction stresses, $\Delta \bar{\sigma}_{r,\theta,z}$ in the plastic range will be defined as follows:

$$\Delta \bar{\sigma}_{r,\theta,z} = (\Delta \sigma_{r,\theta,z})_p - \Delta \sigma_{r,\theta,z} = -(1-e)\Delta \sigma_{r,\theta,z}. \tag{19}$$

The resultant forces of the incremental correction stresses in both tangential and axial directions, Q_θ and Q_z are given respectively by

$$Q_\theta = \int_{\text{(Plastic zone)}} \Delta \bar{\sigma}_\theta \, dr, \qquad Q_z = \int_{\text{(Plastic zone)}} \Delta \bar{\sigma}_z (2\pi r)\, dr.$$

The radial component $\Delta \bar{\sigma}_r$ which vanishes at the elastic-plastic boundary ($e=1$) has no influence on the elastic region. When the inner part of the cross section is plastic and the outer part remains elastic (boundary at $\rho = \rho_e$), the average stresses to be corrected in the elastic region are as follows:

$$\begin{aligned} \Delta \bar{\bar{\sigma}}_r &= 0, \qquad \Delta \bar{\bar{\sigma}}_\theta = -\frac{Q_\theta}{R - r_e} = \frac{\int_0^{\rho_e} (1-e)\Delta \sigma_\theta \, d\rho}{1-\rho_e}, \\ \Delta \bar{\bar{\sigma}}_z &= -\frac{Q_z}{\pi(R^2 - r_e^2)} = \frac{2\int_0^{\rho_e} (1-e)\Delta \sigma_z \rho \, d\rho}{1-\rho_e^2}. \end{aligned} \tag{20}$$

On the other hand, if the inner part is elastic and the outside portion becomes plastic, then

$$\begin{aligned} \Delta \bar{\bar{\sigma}}_r &= 0, \qquad \Delta \bar{\bar{\sigma}}_\theta = -\frac{Q_\theta}{r_e} = \frac{\int_{\rho_e}^{1} (1-e)\Delta \sigma_\theta \, d\rho}{\rho_e}, \\ \Delta \bar{\bar{\sigma}}_z &= -\frac{Q_z}{\pi r_e^2} = \frac{2\int_{\rho_e}^{1} (1-e)\Delta \sigma_z \rho \, d\rho}{\rho_e^2}. \end{aligned} \tag{20'}$$

Finally, the transient stresses in the elastic range, when $\tau = \tau_2$, are given in the following form:

$$\sigma_{r,\theta,z}(\tau = \tau_2) = \sigma_{r,\theta,z}(\tau = \tau_1) + \Delta \sigma_{r,\theta,z} + \Delta \bar{\bar{\sigma}}_{r,\theta,z}. \tag{21}$$

This process of computation will be continued until the temperature of the cylinder becomes uniformly equal to zero. When time approaches infinity ($\tau \to \infty$) the residual stresses are given by the limiting values of Eqs. (16) or (21), depending upon either plastic or elastic regions in the cross section.

d) Numerical Solution

The successive approximation method described in the foregoing articles will be applied to the calculation of the thermal transient and residual stresses in a water-quenched high yield-strength constructional alloy steel cylinder which is subjected to a sudden cooling from a uniform initial temperature ($T_0 = 1300°$ F).

The temperature distribution in the cylinder is computed by Eq. (1) with the constant $c = 4.5$, which is taken from experimental data given in the Ref. (12). Fig. 2 illustrates the results for several values of the time parameter, τ.

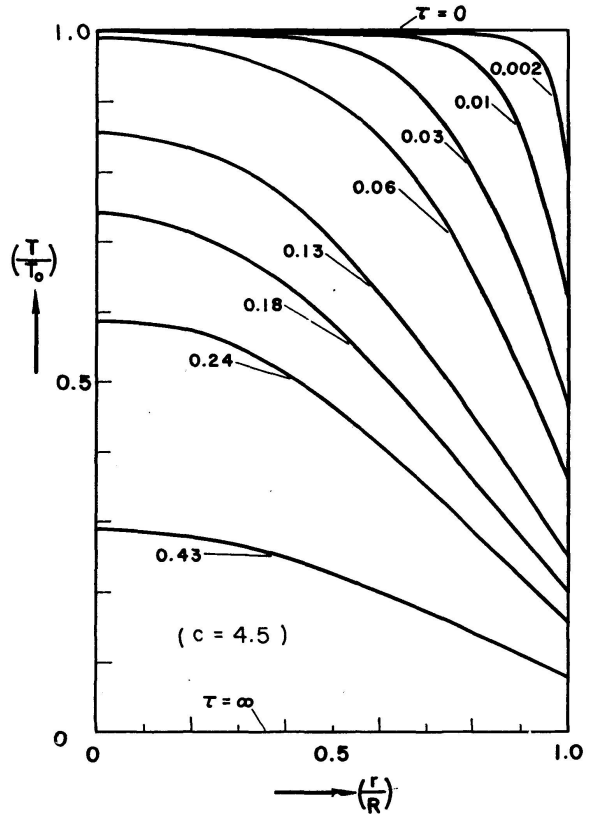

Fig. 2. Temperature distribution in solid circular cylinders.

By using the finite difference method with $N = 10$, the ω_n's are obtained from Eq. (10) for each incremental time interval $\Delta\tau$. The appropriate $E(T)$'s as function of the temperature are taken from Fig. 1b. In this numerical computation it is assumed that the linear coefficient of thermal expansion $\alpha = 7.74 \times 10^{-6}$ inches per inch per degree F is constant throughout the whole range of temperatures according to the results of experimental measurements [13]. It is also assumed that $\nu = 0.3$.

After obtaining the incremental stresses ($\Delta\sigma_r, \Delta\sigma_\theta$ and $\Delta\sigma_z$) from Eq. (11) and summing these stresses, the plasticity condition is checked at every stage of the computation. Then the proper correction is made for elastic-plastic

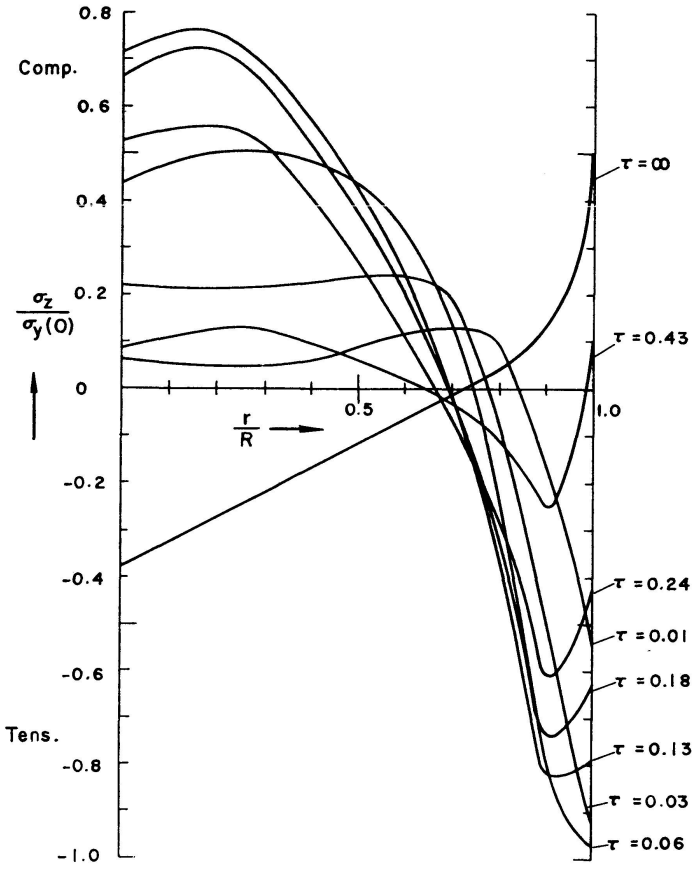

Fig. 3. Thermal transient stress (process of residual stress formation).

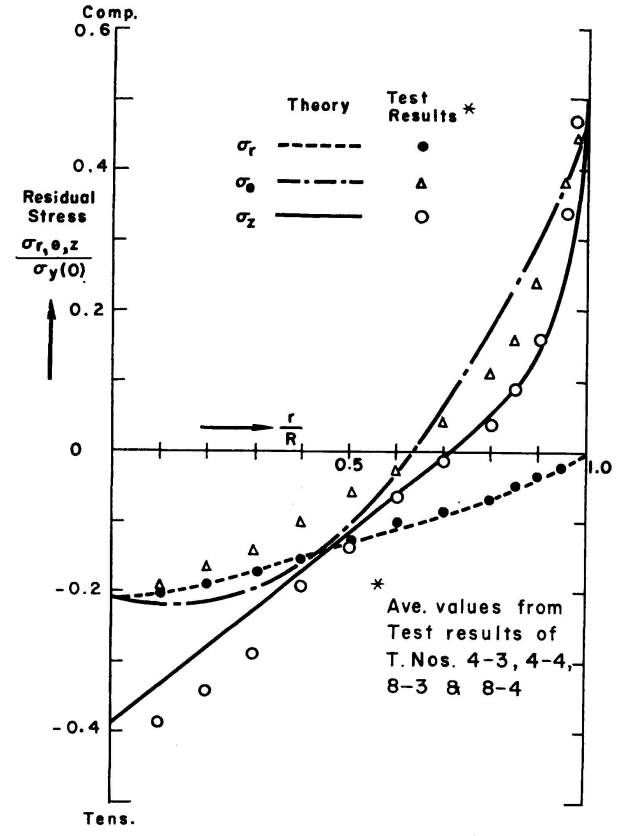

Fig. 4. Residual stresses in quenched steel cylinders.

cases where it is required. This step-by-step process is repeated by evaluating the transient stresses at any instance τ, a typical result being shown in Fig. 3. Finally when $\tau = \infty$, the residual stresses σ_r, σ_θ and σ_z are obtained as demonstrated in Fig. 4.

2. *Experimental Investigation*

Residual stress measurements were carried out on $2^3/_4$ inch diameter specimens of USS "T-1" Steel round bars which were subjected to the following heat treatments: a) quench, temper and stress-relieve, b) quench, temper and air-cool, and c) quench, temper and quench from the tempering temperature [14]. Of these, the quench, temper and air-cool treatment is the normal production treatment.

Since in circular cylindrical bars the residual stresses resulting from heat treatment can be assumed to have a distribution pattern of polar symmetry, Sachs' method is regarded as a suitable way for the measurement of the triaxial residual stresses [15]. It should be pointed out, however, that the ordinary boring-out operation might cause yielding of the material adjacent to the drilled layer due to the heat generated. Thereby unexpected influences may be introduced on the strain measurements. Such influences can be considered as local effects and hence safely ignored only if the strain readings are made on surfaces sufficiently removed from the bored layer. They do become serious when the drilling layer approaches the outer surface where the strain gages are attached. To avoid these unfavorable conditions and to obtain the complete residual stress pattern including the outer part of the cross section, which gives the largest contribution to the bending rigidity of the member, and thereby to its column strength, the so-called "combined method" [16] together with the "boring-out method" was used in this series of experiments. Two test specimens taken from originally identical material were measured by these two different methods. The results obtained from these independent tests were checked against each other in that region of the cross section where both methods were applied.

As can be seen from the derivation of Sachs' equation, if only the boring-out method is used, the equilibrium condition of resulting forces over the entire cross section is always satisfied regardless of whether the measured magnitude and distribution of residual stresses is correct or not. Consequently, the equilibrium condition is not sufficient to check the test results. If, however, two independent processes such as the boring-out method and the combined method are used on two specimens taken from identical material, it is then possible to perform the equilibrium check in the final results of the residual stress distribution. The difference between the computed tensile and compressive resultant forces were in all cases of this series less than five percent.

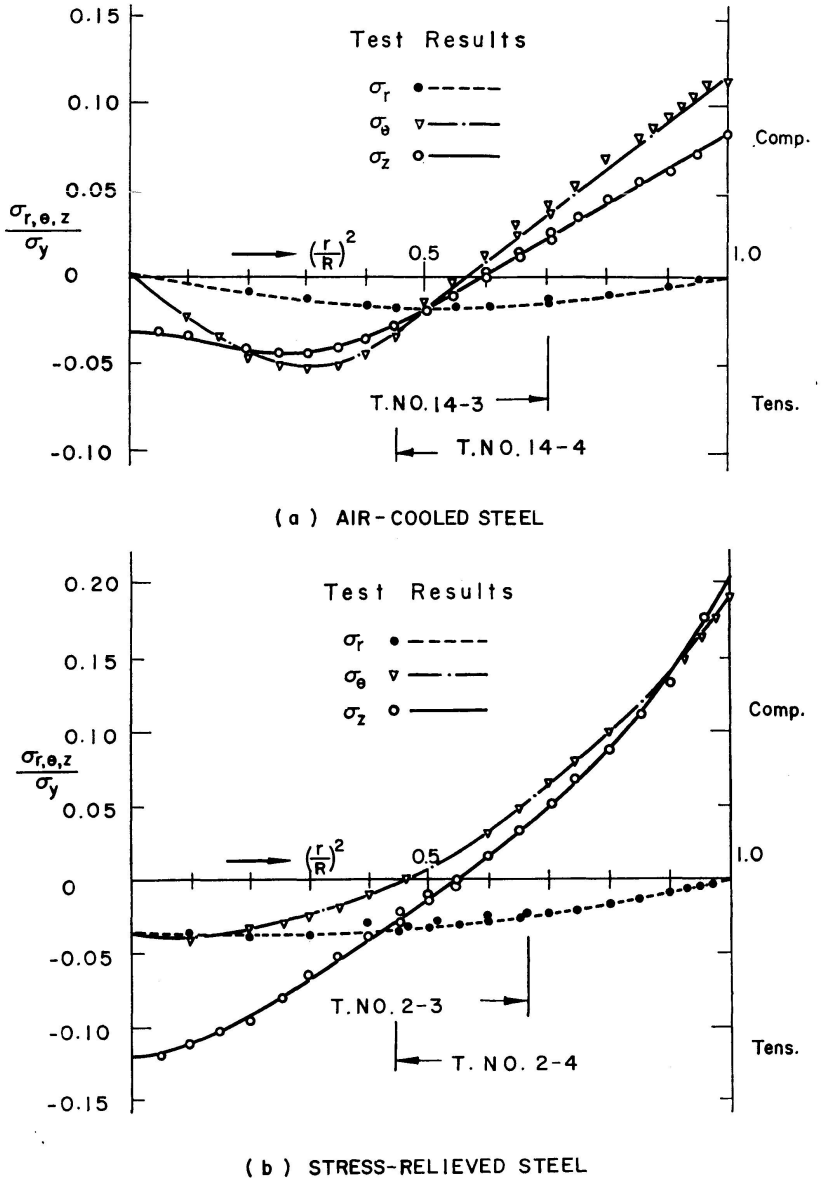

Fig. 5a), b). Measured residual stresses in air-cooled or stress-relieved steel cylinders.

The experimentally determined residual stresses for bars that were water-quenched from the tempering temperature after tempering are shown in Fig. 4 and are compared with the theoretical values obtained by the analytical method presented in the previous article. Their correlation is satisfactory.

In addition measured residual stresses for an air-cooled and a stress-relieved material are shown in Figs. 5a and 5b indicating a considerable decrease in the magnitude of residual stresses from the one observed in the quenched material.

III. Inelastic Buckling Strength of Circular Columns

1. Column Strength and the "Equivalent Residual Stress"

Since the column strength in the inelastic range is dependent upon the magnitude and distribution of the residual stresses, it is necessary to calculate the strength for each case of a given shape of cross section with a known pattern of residual stress. For steel columns of wide-flange shape or rectangular cross section, reasonable solutions were obtained theoretically. They were checked with a large number of tests [5]. The residual stress in these columns is practically uniaxial so that the total stress at any fiber in the cross section can be obtained simply as the sum of the residual stress and the imposed stress due to loading.

In the case of solid circular columns, however, it has been found that the residual stresses due to heat treatment are triaxial, and the axial and tangential stresses have almost the same magnitude at the outer surface of the cross section. Therefore, some consideration must be given to the effect of the triaxiality of the residual stresses on column strength. For convenience a fictitious longitudinal residual stress called the "equivalent residual stress", σ_e will be introduced into the analysis to avoid dealing with the actual triaxial state present in the member. This stress will be defined such that the yield condition can be expressed simply by the following equation as in the uniaxial case:

$$\sigma_e + \sigma = \sigma_y, \tag{22}$$

where σ is the compressive stress due to an applied load.

When a cylindrical column, which contains residual stresses σ_r, σ_θ and σ_z is subjected to an additional axial compressive stress, σ, yielding will take place at points where Mises' yield condition is satisfied:

$$\tfrac{1}{6}\left[\{(\sigma+\sigma_z)-\sigma_\theta\}^2+\{\sigma_\theta-\sigma_r\}^2+\{\sigma_r-(\sigma+\sigma_z)\}^2\right]=\tfrac{1}{3}\sigma_y^2\,. \tag{23}$$

From Eqs. (22) and (23), the "equivalent residual stress" is expressed by the following formula:

$$\sigma_e=\sigma_z-\tfrac{1}{2}(\sigma_\theta+\sigma_r)+\sigma_y-\sqrt{\sigma_y^2-\tfrac{3}{4}(\sigma_\theta-\sigma_r)^2}\,. \tag{24}$$

Using the static yield stress of the material determined from coupon tests and the residual stresses determined in the previous chapter of this paper, the equivalent residual stresses in each column member can be computed.

Thus, the equivalent residual stress pattern shown by the dashed line in Fig. 6 was determined. For convenience in making subsequent calculations the following equation was assumed to approximate this pattern:

$$\frac{\sigma_e(\rho)}{\sigma_y}=a\,\rho^n+b\,. \tag{25}$$

The three constants, a, b and n can be selected such that the actual results are best approximated in a chosen region. As will be discussed in the following articles, the closer the approximation is at the outer part of the cross section (which contributes most to column strength and also usually contains the highest compressive residual stresses), the better will be the column strength

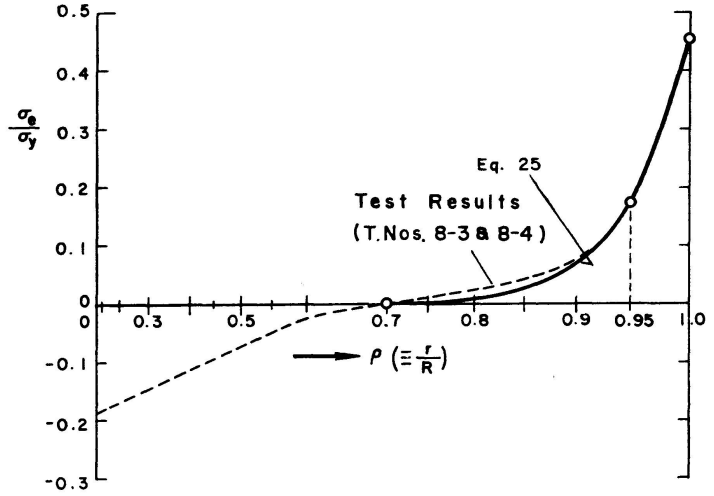

Fig. 6. Equivalent residual stress.

prediction. In the case of an as-quenched material, for example, the constants were obtained by matching the analytical expression, Eq. (25) with the equivalent residual stress at $\rho = 0.70$, 0.95 and 1.00. The resulting constants were

$$a = 0.459, \qquad b = 0, \qquad n = 19.0,$$

Fig. 6 shows the comparison between the actual equivalent residual stress distribution and this approximation, which is only valid for the outer part of the cross section. A better representation of the equivalent residual stresses over the entire cross section can be achieved by introducing lower order terms of ρ. However, as will be shown in the following chapter, the effect of using more involved expressions in the computation of the ultimate strength of a column is negligible except for very short columns. Columns of practical length reach their maximum load before yielding penetrates into the region $\rho < 0.5$ where the magnitude of the equivalent residual stress is usually low.

2. Stress-Strain Relationship for Coupons and for Stub Columns

The most fundamental basis for the determination of the inelastic buckling strength of column members is the static stress-strain relationship of the material in the inelastic range. This relationship can only be obtained from coupon tests which are conducted under a controlled rate of strain [17], and

is not affected by residual stresses. For a high-strength constructional alloy steel, such as USS "T-1" steel, the stress-strain curve of a coupon shows a pronounced yield stress level and strain hardening can hardly be observed until fracture takes place [14]. In other words, the idealized elastic-fully plastic stress-strain relationship is a good approximation for such an alloy steel and will be used in the analysis that follows.

The average stress-strain relationship for a short (stub) column, which is affected by residual stresses, can be used to predict the buckling strength of long or intermediate length columns of the same material and cross section. When such a stub column is subjected to compression, yielding will start from the outer part of the cross section, where a relatively high residual stress in compression is present. If the distribution pattern of the equivalent residual stress is polar symmetric, $\sigma_e(r)$, then the boundary between an elastic core and the yield zone is a concentric circle. Letting the radius of this circle be r_e, the average compressive stress, σ_{ave}, and the average strain, ϵ_{ave}, due to the imposed loading are given by the following equations:

$$\sigma_{ave}(r_e) = \sigma_y - \left(\frac{r_e}{R}\right)^2 \sigma_e(r_e) - \frac{2}{R^2}\int_{r_e}^{R} r\,\sigma_e(r)\,dr, \tag{26}$$

$$\epsilon_{ave}(r_e) = \frac{1}{E}\{\sigma_y - \sigma_e(r_e)\}. \tag{27}$$

Thus, for a given pattern of the equivalent residual stress the average stress-strain relationship of a bar containing residual stresses is readily obtained by

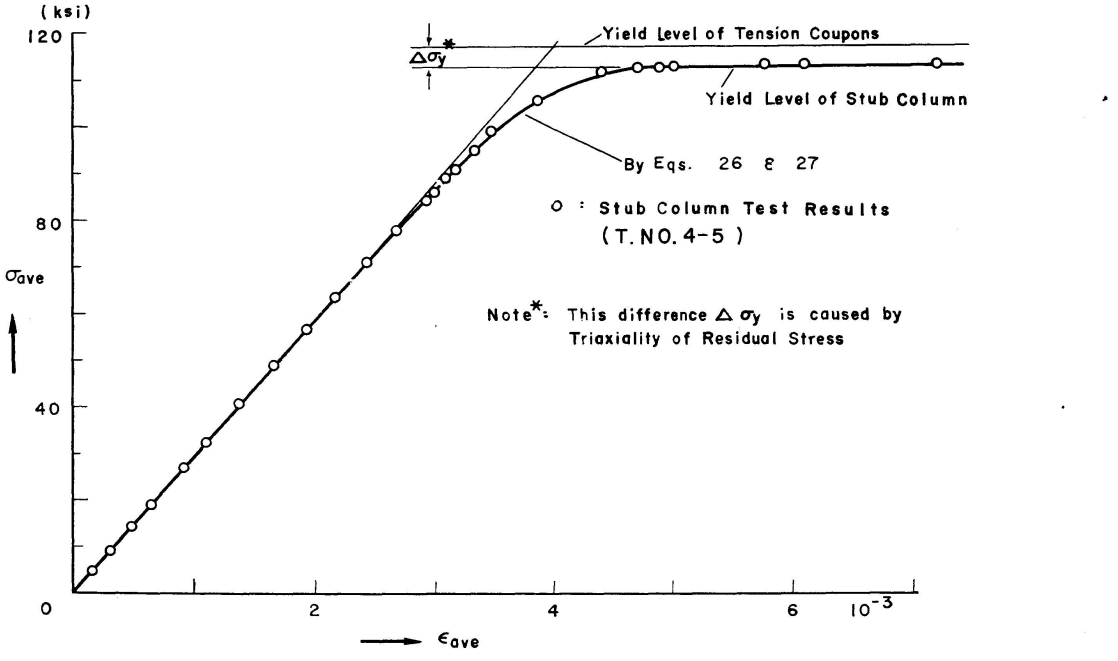

Fig. 7. Average stress-strain diagram.

eliminating r_e from Eqs. (26) and (27). Fig. 7 is an example of this relationship, and shows fairly good agreement with the stub column test results [14].

Since the resultant force determined by integrating the equivalent residual stress over the entire cross section does not necessarily vanish, it should be anticipated that the yield level predicted from coupon test results will not necessarily coincide with that determined from the stub column test. Fig. 7 shows that this is actually the case. The difference between these two values is due to the effect of the triaxiality of the residual stresses in the solid cylindrical column. In the case of an as-quenched material, for example, the difference was found to be about four percent.

3. Tangent Modulus Load

According to the tangent modulus theory, the buckling load, P_{cr}, of a centrally loaded and perfectly straight column is given by the so-called tangent modulus formula [18]:

$$\frac{P_{cr}}{A} = \frac{\pi^2 E_t}{\left(\frac{k L}{r_0}\right)^2}$$

in which A is the cross sectional area, $\frac{k L}{r_0}$ is the effective slenderness ratio, and E_t is the tangent modulus of the material. This formula presumes that the material is homogeneous even in the inelastic range and that its stress-strain characteristic is known.

If, however, residual stresses are present in a column member compressed beyond the elastic limit, yielding will take place at localized parts of the cross section where the total stress is equal to σ_y. Thereafter, the column material becomes non-homogeneous. When an idealized stress-strain relationship is assumed for the material and residual stresses are taken into account, the following formula for the buckling load, P_{cr} applies [4]:

$$\frac{P_{cr}}{A} = \frac{\pi^2 E}{\left(\frac{k L}{r_0}\right)^2} \frac{I_e}{I}, \tag{28}$$

where $E I_e$ is the effective bending rigidity of the column, E being the modulus of elasticity of the material and I_e being the moment of inertia of the elastic portion of the cross section.

When a perfectly straight circular cylindrical column, containing relatively high compressive equivalent residual stresses of a polar symmetric distribution is subjected to a monotonically increasing axial thrust, yielding will start from the surface. As has been discussed in the foregoing article, the elastic core will

be bounded by a concentric circle having a radius, r_e. Resistance to bending of such a cross section is dependent on the moment of inertia of the elastic core if no strain-reversal occurs at the instance of bending, as is assumed in the tangent modulus concept. Non-dimensionalized for the present problem the moment of inertia is:

$$\frac{I_e}{I} = \left(\frac{r_e}{R}\right)^4. \tag{29}$$

Using the average stress-strain relationship expressed by Eqs. (26) and (27) in the preceding article, the tangent modulus of a stub column, E_t can be obtained in the following manner:

$$E_t = \frac{d\,\sigma_{ave}}{d\,\epsilon_{ave}} = E\left(\frac{r_e}{R}\right)^2. \tag{30}$$

Eq. (28) can therefore be written as follows:

$$\frac{P_t}{A} = \frac{\pi^2 E}{\left(\frac{k\,L}{r_0}\right)^2}\left(\frac{E_t}{E}\right)^2. \tag{31}$$

It should be noted that this new formula gives a lower prediction of the buckling load than that based on the conventional tangent modulus theory.

4. Reduced Modulus Load

Another criterion used to define the buckling load of a perfectly straight column subjected to a concentric axial thrust is the "reduced modulus load". This load, P_r, is defined as the load at which the member is, at least theoretically, not stable but is indifferent with regard to a deformed position. Moreover, the reduced modulus concept assumes that the column member remains absolutely straight until the reduced modulus load is applied. Although practical columns rarely behave in this assumed manner, the reduced modulus concept is useful because it gives an upper limit to the load-carrying capacity of a member.

It is assumed that the simplified stress-strain relationship shown in Fig. 8a is applicable to any fiber, that the column is kept perfectly straight until the axial thrust reaches the reduced modulus load, P_r, and that yielding in any cross section along the member penetrates to $r=r_e$. (Fig. 8b and 8c.) At the instance when the reduced modulus load is reached, a bending moment, ΔM induced by an infinitesimally small increment of curvature, $\Delta\Phi$, is computed in the following manner (strain reversal being allowed):

$$\Delta M = \int \Delta\sigma\,(x-s)\,dA, \tag{32}$$

where s is the distance from the centroidal axis to an assumed neutral axis in the cross section. $\Delta\sigma = E\,\Delta\Phi\,(x-s)$ in the region of either the elastic core ($r \leqq r_e$) or unloading zone. On the other hand, $\Delta\sigma = 0$ for a loading zone of $r > r_e$. The calculation is carried out for two possible cases (as shown in Fig. 8) depending upon the assumed position of the neutral axis; i.e. for $s \geqq r_e$, and for $s \leqq r_e$.

The effective rigidity, $E\,I_e$, against the infinitesimally small bending is

$$E\,I_e = \frac{\Delta M}{\Delta \Phi}. \tag{33}$$

The resulting non-dimensionalized formulæ are:

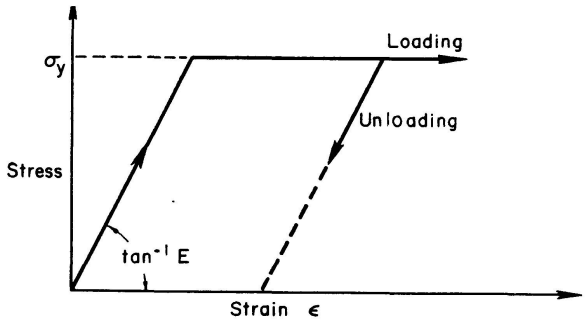

(a) STRESS-STRAIN RELATIONSHIP

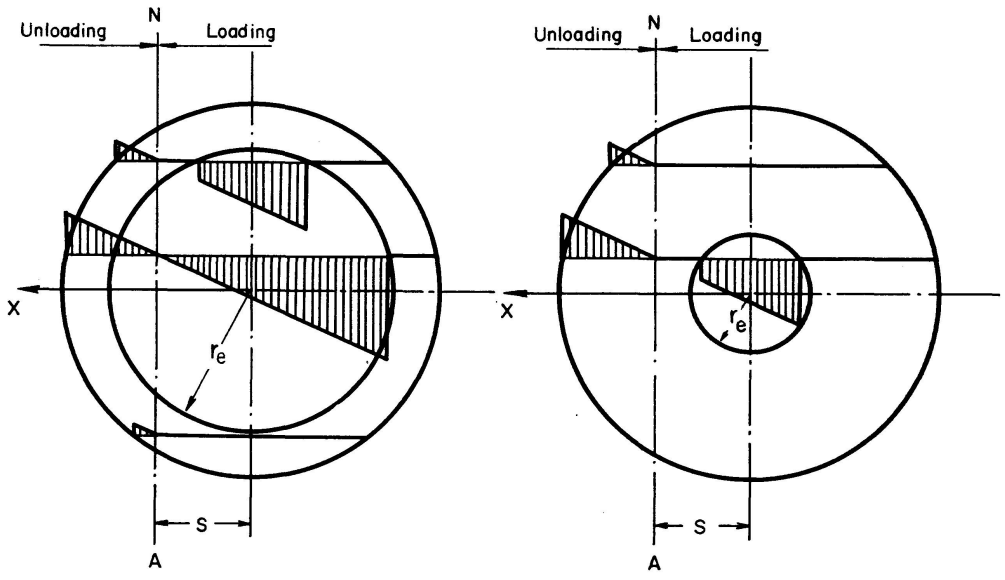

(b) $s \leqslant r_e$ (c) $s \geqslant r_e$

Fig. 8a), b), c). Pattern of stress increment at reduced modulus load.

$$\frac{I_e}{I} = \frac{1}{\pi}\left[\rho_e^2(\rho_e^2+4\bar{s}^2)\left(\pi-\cos^{-1}\frac{\bar{s}}{\rho_e}\right)+(1+4\bar{s}^2)\cos^{-1}\bar{s}\right]$$
$$-\frac{\bar{s}}{3\pi}[\sqrt{1-\bar{s}^2}\,(13+2\bar{s}^2)-\sqrt{\rho_e^2-\bar{s}^2}\,(13\rho_e^2+2\bar{s}^2)], \qquad (\text{for } \bar{s}\leqq\rho_e),$$

$$\frac{I_e}{I} = \frac{1}{\pi}[\pi\rho_e^2(\rho_e^2+4\bar{s}^2)+(1+4\bar{s}^2)\cos^{-1}\bar{s}] \qquad (34)$$
$$-\frac{\bar{s}}{3\pi}\sqrt{1-\bar{s}^2}\,(13+2\bar{s}^2), \qquad (\text{for } \bar{s}\geqq\rho_e),$$

where $$\rho_e \equiv \frac{r_e}{R} \quad \text{and} \quad \bar{s} = \frac{s}{R}.$$

The position of the neutral axis, $\bar{s}$, is determined by the condition that there shall be no increment in the axial thrust, P, that is

$$\Delta P = \int \Delta\sigma\, dA = 0. \qquad (35)$$

Hence
$$\tfrac{1}{3}\sqrt{\rho_e^2-\bar{s}^2}\,(2\rho_e^2+\bar{s}^2)+\rho_e^2\bar{s}\left(\pi-\cos^{-1}\frac{\bar{s}}{\rho_e}\right)-\rho_e\bar{s}^2\sin\left(\cos^{-1}\frac{\bar{s}}{\rho_e}\right)$$
$$-\tfrac{1}{3}\sqrt{1-\bar{s}^2}\,(2+\bar{s}^2)+\bar{s}\cos^{-1}\bar{s}=0, \qquad (\text{for } \bar{s}\leqq\rho_e), \qquad (36)$$
$$\pi\rho_e^2\bar{s}-\tfrac{1}{3}\sqrt{1-\bar{s}^2}\,(2+\bar{s}^2)+\bar{s}\cos^{-1}\bar{s}=0, \qquad (\text{for } \bar{s}\geqq\rho_e).$$

These equations were solved graphically for given values of ρ_e, and the results are shown in Fig. 9.

By using these results, I_e/I will be obtained from Eq. (34). In Fig. 10, it can be seen that the effective bending rigidity, I_e/I, based upon the reduced modulus concept is approximately proportional to $(r_e/R)^2$, whereas that corresponding to the tangent modulus theory is proportional to $(r_e/R)^4$. Therefore,

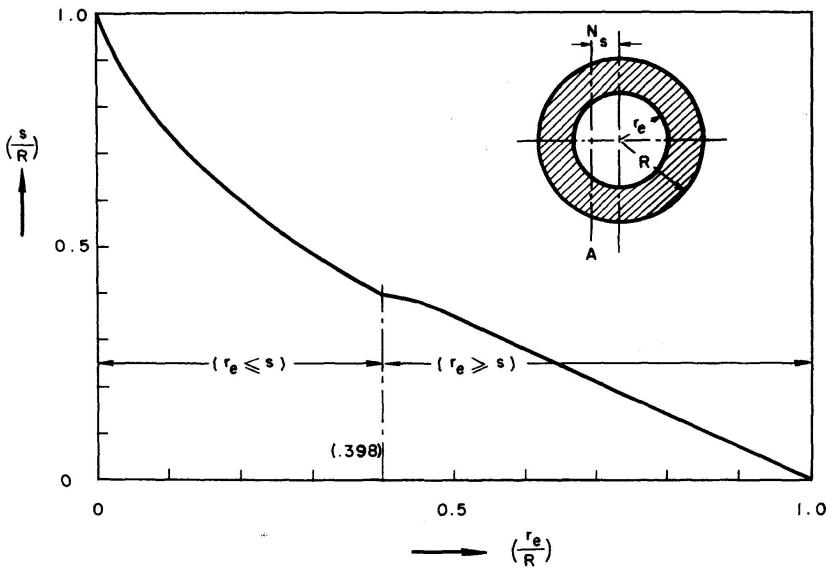

Fig. 9. Position of neutral axis at reduced modulus load.

from Eqs. (28) and (30) it follows that the reduced modulus load, P_r, can be expressed as follows:

$$\frac{P_r}{A} \cong \frac{\pi^2 E}{\left(\frac{kL}{r_0}\right)^2} \frac{E_t}{E}. \tag{37}$$

It is interesting to note that the conventional formula for the buckling load which has been regarded as the "tangent modulus load" is found, by considering the influence of residual stresses, to be approximately equal to the "reduced modulus load" in the case of columns with circular cross sections. The "true tangent modulus load" i.e. the load in case of no strain reversal, is given by Eq. (31). The difference between the two values for the as-quenched column, is less than seven percent [14].

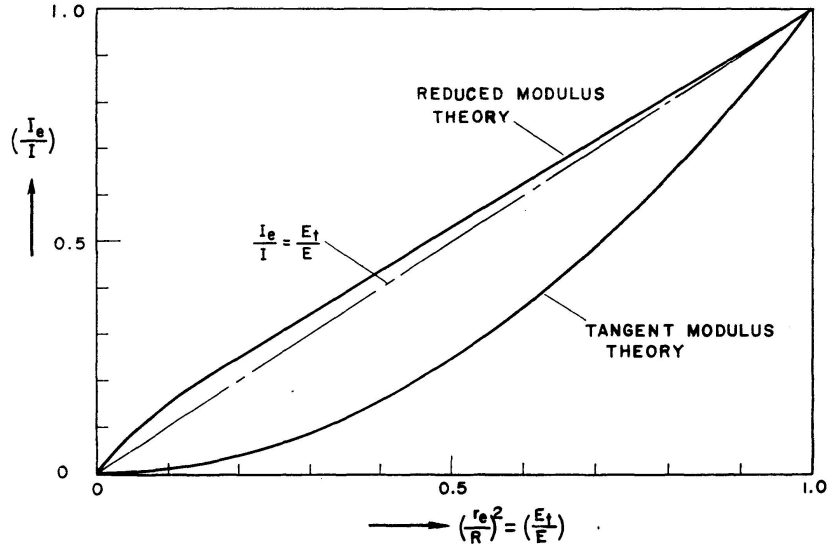

Fig. 10. Effective bending rigidity.

IV. Ultimate Strength of Circular Columns

1. General

A determination of the true ultimate strength of columns is a post-buckling problem. A general analytical solution to this problem is extremely difficult to obtain because the yield pattern over the cross section and consequently the bending rigidity for inelastic columns is a function not only of loads and curvatures at each instance but also of the magnitude and distribution of the residual stresses present in the members. It is therefore unrealistic to investigate the ultimate strength of a column by calculating the bending rigidity of the partially yielded cross section by using a stress-strain relationship of the material from a coupon test without considering residual stresses. In this paper a semi-graphical approach taking into account the effect of the residual

stresses for obtaining a solution to the ultimate load-carrying capacity of circular columns will be presented.

Although there might be other factors reducing the ultimate load-carrying capacity of concentrically loaded columns, the effect of initial deflections of members will be of major significance [19]. For this reason, investigations on the combined effects of these internal and external imperfections, that is "residual stresses" and "out-of-straightness", will be carried out.

The following assumptions are made in determining the ultimate strength of a simply supported column of length $k\,L$ subjected to an axial compressive load.

1. The material possesses the idealized elastic-fully plastic type of stress-strain relationship. (See Art. III. 2.)
2. Plane cross sections remain plane.
3. Mises' yield condition defines the yielding of the material. (See Art. III. 1.)
4. Lateral deflections of the column can be approximated by a cosine curve,

$$u(z) = d\cos\left(\frac{\pi z}{k\,L}\right),$$

where d is the deflection at mid-length of the column. Hence it follows that the curvature, Φ, at that point is expressed as (see Art. IV. 4):

$$d = \left(\frac{k\,L}{\pi}\right)^2 \Phi. \tag{38}$$

The column strength can be best investigated by observing the behavior at the most critical section of the member, that is, at mid-length of the column. If a circular column containing an equivalent residual stress, σ_e, is subjected to an axial compressive load, yielding will start when the sum of the applied compressive stress and the equivalent residual stress at any point on the cross section reaches the yield stress of the material. Further application of loading produces an elastic-plastic cross section. For simplicity, the stress, σ, due to the applied load may be divided into two parts: a) a linear distribution, σ_l: b) a correction pattern for the yielded zone, $\bar{\sigma}$ (Fig. 11). The applied stress in the cross section, then, can be expressed in the following way:

In the elastic region,

$$\sigma = \sigma_l, \quad (\text{for } \sigma + \sigma_e < \sigma_y). \tag{39}$$

In the plastic region,

$$\sigma = \sigma_l - \bar{\sigma}, \quad (\text{for } \sigma + \sigma_e = \sigma_y). \tag{40}$$

Letting σ_0 be a stress at the center of the cross section, it can be shown that

$$\sigma_l = \sigma_0 + E\,\Phi\, r\cos\theta. \tag{41}$$

Furthermore, the elastic-plastic boundary in the cross section is given by the equation:

$$\sigma_e + \sigma_l = \sigma_y. \tag{42}$$

Now the axial thrust, P, applied to the column is readily computed from the equilibrium consideration:

$$P = \int \sigma \, dA = \sigma_0 A - \int_{\text{(Plastic zone)}} \bar{\sigma} \, dA . \tag{43}$$

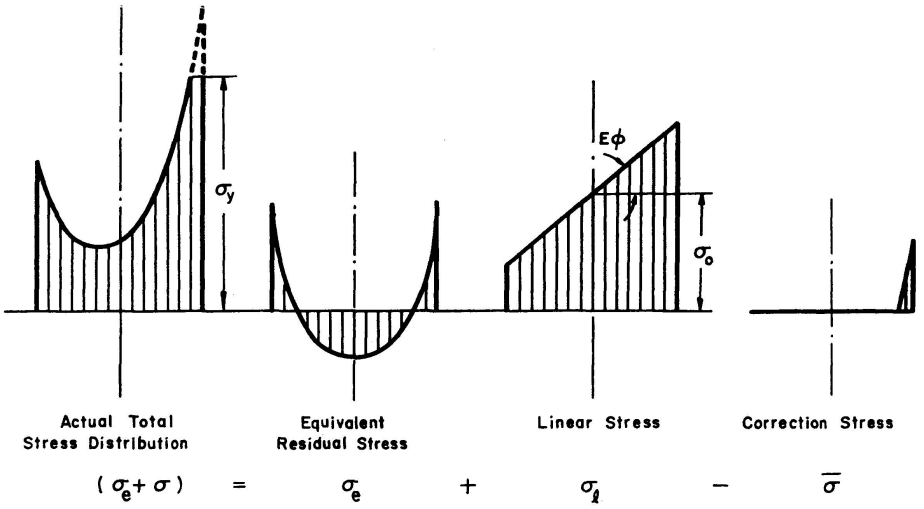

Fig. 11. Stress pattern in cross section.

Also, the internal moment, M, about the centroidal axis at the cross section in question is given by:

$$M = \int \sigma r \cos\theta \, dA = E I \Phi - \int_{\text{(Plastic zone)}} \bar{\sigma} r \cos\theta \, dA . \tag{44}$$

By introducing non-dimensional parameters, λ and φ, defined as

$$\lambda \equiv \frac{\sigma_0}{\sigma_y} \quad \text{and} \quad \varphi \equiv \frac{E R}{\sigma_y} \Phi$$

the elastic-plastic boundary (Eq. (42)) may be given as

$$\lambda + \varphi \rho \cos\theta - 1 + \frac{\sigma_e}{\sigma_y} = 0 . \tag{42'}$$

Similarly, P and M are obtained, by using Eqs. (40) and (41), as follows:

$$\frac{P}{P_y} = U(\lambda, \varphi) = \lambda - \frac{1}{\pi} \iint_{\text{(Plastic zone)}} \left[\lambda + \varphi \rho \cos\theta - 1 - \frac{\sigma_e}{\sigma_y} \right] \rho \, d\rho \, d\theta . \tag{43'}$$

$$\frac{M}{P_y R} = V(\lambda, \varphi) = \frac{\varphi}{4} - \frac{1}{\pi} \iint_{\text{(Plastic zone)}} \left[\lambda + \varphi \rho \cos\theta - 1 - \frac{\sigma_e}{\sigma_y} \right] \rho^2 \cos\theta \, d\rho \, d\theta . \tag{44'}$$

If the pattern of the equivalent residual stress, σ_e/σ_y is given, the elastic-plastic boundary is obtained as a solution of Eq. (42'). Herewith, $U(\lambda, \varphi)$ and $V(\lambda, \varphi)$ can be computed by Eqs. (43') and (44'), respectively.

At mid-length of the column, the following relationship must be satisfied.

$$M = P(d_0 + d), \tag{45}$$

where

d_0 = initial lateral deflection at mid-length of the column, and
d = additional lateral deflection at the same point.

From Eq. (38),

$$\frac{d}{R} = \frac{\eta^2}{4}\varphi,$$

where

$$\eta \equiv \frac{\left(\frac{kL}{r_0}\right)}{\pi\sqrt{\frac{E}{\sigma_y}}} \qquad \text{(generalized slenderness ratio of column)}.$$

Hence Eq. (45) can be given in the following form:

$$\frac{V(\lambda, \varphi)}{U(\lambda, \varphi)} = \frac{d_0}{R} + \frac{\eta^2}{4}\varphi. \tag{45'}$$

This equation determines the relationship between λ and φ for a given column (given values of d_0/R and η). It may be solved by a graphical method. Using this particular set of λ and φ, P/P_y will be computed from Eq. (43'), and thereby the load-deflection curves can be obtained.

2. Columns with Residual Stresses of Polar Symmetry

When a column member contains a polar symmetric residual stress pattern such as caused by heat treatments, the load carrying capacity of the member can be obtained from the results of the previous article by using the assumed equivalent residual stress pattern, $\sigma_e(\rho)$ of Eq. (25).

It can be seen from Eq. (39), that the cross section of the member remains in a fully elastic state as long as the following relationship between λ and φ is satisfied:

$$0 \leqq \lambda \leqq (1-a-b)-\varphi. \tag{46}$$

When comparatively high compressive equivalent residual stresses exist at the surface of the cross section, yielding can produce the two different patterns shown in Fig. 12. The proper choice of these two patterns for an elastic-plastic case depends on the following relations:

Elastic-plastic case A:

$$(1-a-b)-\varphi \leqq \lambda \leqq (1-a-b)+\varphi. \tag{47}$$

Elastic-plastic case B:

$$(1-a-b)+\varphi \leqq \lambda. \tag{48}$$

From Eq. (42′) the boundary between the elastic core and the plastic zone is given by the following equation.

$$a\rho^n + \varphi\rho\cos\theta + (\lambda + b - 1) = 0. \tag{49}$$

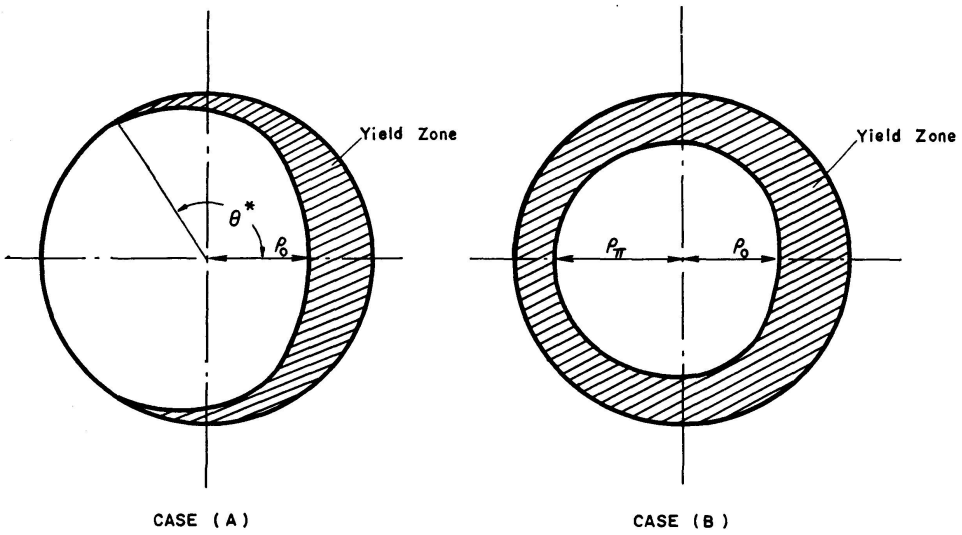

Fig. 12. Yield pattern in cross section.

To simplify the integrations in Eqs. (43′) and (44′) it will be assumed that this boundary line can be approximated by the following expression:

$$\rho(\theta) = \rho_0 \exp(\mu\theta) \tag{50}$$

where ρ_0 and μ are independent of the coordinates, ρ and θ, and can be determined in the following manner:

Case A:

At $\theta = 0$, $\rho = \rho_0$ which is a root of the equation

$$a\rho^n + \varphi\rho + (\lambda + b - 1) = 0 \tag{51}$$

and the limiting angle, θ^*, for the boundary line at $\rho = 1$ (see Fig. 12) is given by

$$\theta^*(\lambda, \varphi) = \cos^{-1}\left(\frac{1 - a - b - \lambda}{\varphi}\right). \tag{52}$$

Furthermore,

$$\mu(\lambda, \varphi) = -\frac{\log_e \rho_0}{\theta^*}. \tag{53}$$

Case B:

ρ_0 is obtained from Eq. (51) in the same way as in Case A. At $\theta = \pi$, $\rho = \rho_\pi$, which is determined as a root of the equation

$$a\rho^n - \varphi\rho + (\lambda + b - 1) = 0. \tag{54}$$

Furthermore,

$$\mu(\lambda, \varphi) = \frac{1}{\pi} \log_e \left(\frac{\rho_\pi}{\rho_0} \right). \tag{55}$$

With this information on the elastic-plastic boundary in the cross section, $U(\lambda, \varphi)$ and $V(\lambda, \varphi)$ are obtained:

$$\begin{aligned} U(\lambda, \varphi) = \lambda &+ \left[\frac{2a}{(n+2)^2 \mu \pi} \right] \begin{Bmatrix} [1 - \rho_0^{n+2}] \\ [\rho_\pi^{n+2} - \rho_0^{n+2}] \end{Bmatrix} - \left[\frac{1-b-\lambda}{2\mu\pi} \right] \begin{Bmatrix} [1 - \rho_0^2] \\ [\rho_\pi^2 - \rho_0^2] \end{Bmatrix} \\ &+ \left[\frac{1}{\pi} \left(1 - \frac{2a}{n+2} - b - \lambda \right) \right] \begin{Bmatrix} \theta^* \\ \pi \end{Bmatrix} - \left[\frac{2\mu\varphi}{\pi(1+9\mu^2)} \right] \begin{Bmatrix} [3\mu \sin\theta^* - \cos\theta^* + \rho_0^3] \\ [\rho_\pi^3 + \rho_0^3] \end{Bmatrix}, \end{aligned} \tag{56}$$

$$\begin{aligned} V(\lambda, \varphi) = &\left[\frac{\varphi}{4} \right] \begin{Bmatrix} \left[1 - \dfrac{\theta^*}{\pi} \right] \\ [0] \end{Bmatrix} - \left[\frac{2a\mu}{\pi\{1+(n+3)^2\mu^2\}} \right] \begin{Bmatrix} [(n+3)\mu \sin\theta^* - \cos\theta^* + \rho_0^{n+3}] \\ [\rho_\pi^{n+3} + \rho_0^{n+3}] \end{Bmatrix} \\ &+ \left[\frac{\varphi}{16\pi\mu(1+4\mu^2)} \right] \begin{Bmatrix} [1 + 8\mu^2(\cos^2\theta^* - \mu \sin 2\theta^*) - (1+8\mu^2)\rho_0^4] \\ [(1+8\mu^2)(\rho_\pi^4 - \rho_0^4)] \end{Bmatrix} \\ &+ \left[\frac{2\mu(1-b-\lambda)}{\pi(1+9\mu^2)} \right] \begin{Bmatrix} [3\mu \sin\theta^* - \cos\theta^* + \rho_0^3] \\ [\rho_\pi^3 + \rho_0^3] \end{Bmatrix}. \end{aligned} \tag{57}$$

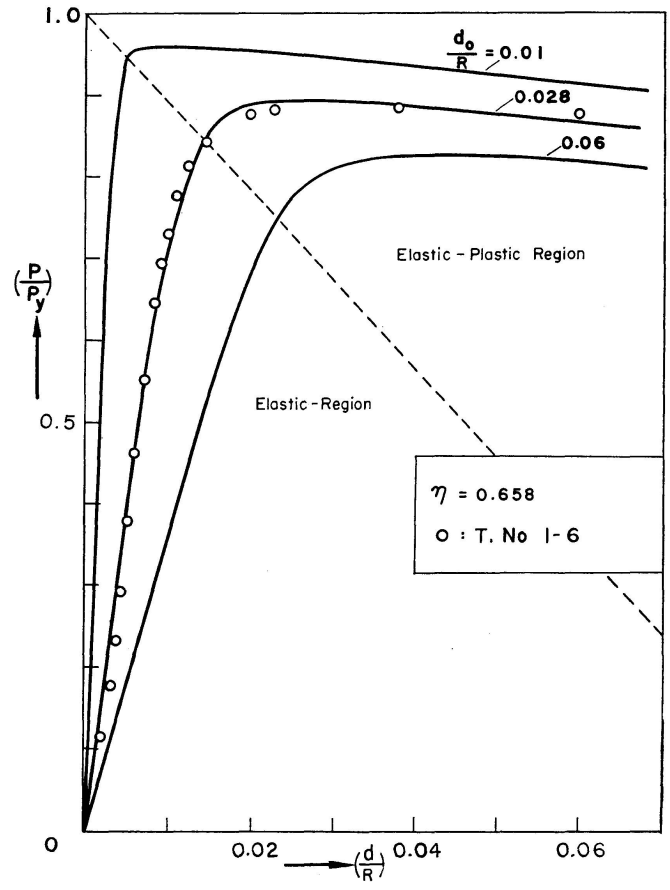

Fig. 13. Load-deflection curves of axially loaded column (without residual stress).

The upper term in brackets, $\{\}$, is for Case A, and the lower term is for Case B. It can be easily seen that for an elastic case, $U=\lambda$, $V=\varphi/4$.

For an assumed value of φ, the corresponding value of λ can be determined from Eqs. (45′), (56) and (57) by means of a graphical method. The value of P/P_y will then be obtained from Eq. (56).

Typical results of the load-deflection curves for columns without and with residual stresses are shown in Fig. 13 and Fig. 14, respectively. The behavior of an initially straight column is illustrated by the load-deflection diagram for $d_0=0$ in Fig. 14. It was observed from the computation that strain reversal starts to take place after exceeding the true tangent modulus load, where the yield pattern in the cross section (Case B) changes its shape gradually, and eventually turns into Case A. The maximum load the member can carry is slightly higher than the true tangent modulus load, the difference between these two loads being dependent upon the slenderness ratio of the column.

Fig. 15 indicates both the effects of initial deflections and residual stresses of polar symmetry on the ultimate strength of column members. It can be seen from the figure that a considerable loss in the ultimate load-carrying capacity must be anticipated for columns with even a small amount of initial deflection. This is especially pronounced in the range $\eta=1.0$.

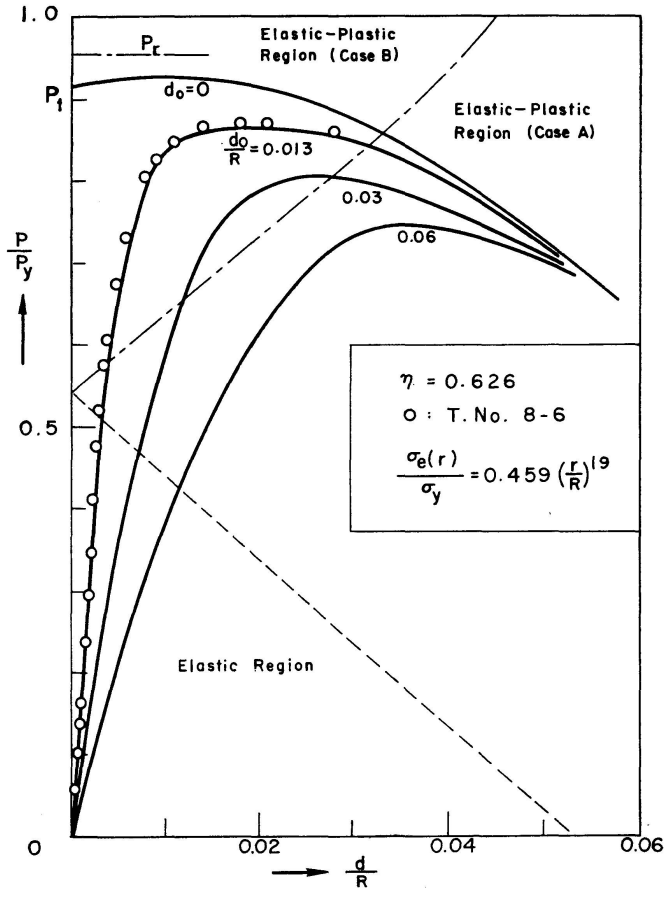

Fig. 14. Load-deflection curves of axially loaded column (including residual stress).

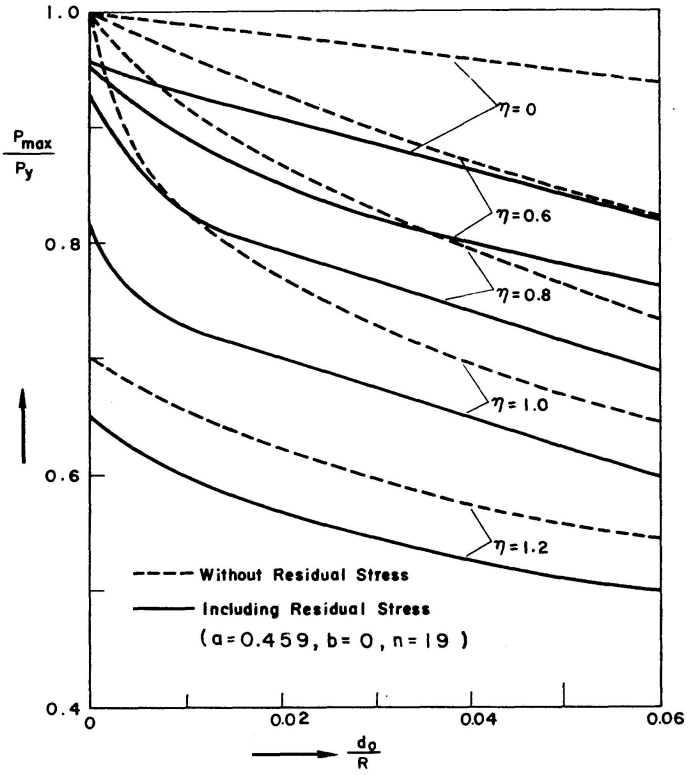

Fig. 15. Ultimate strength of circular columns without/and including residual stress of polar symmetry.

3. *Experimental Verification of the Theory*

Concentrically loaded column tests were performed [14] to verify the theoretical predictions of the ultimate strength of high yield strength alloy steel round columns developed in this paper.

As shown in Fig. 16, the columns were tested in a flat-ended condition. The effective length, $k\,L$, was determined by measuring the locations of zero curvature directly with strain gages. It was therefore unnecessary to consider the effects of unavoidable end eccentricities upon the column strength. To determine the initial deflection of the members, precise measurements in two perpendicular directions were made on each specimen.

First, to check the relationship between deflection and curvature at mid-height of the column assumed in Art. IV. 1, test results of these values compared with Eq. (38). Fig. 17 shows that this assumption is satisfactory.

The column behavior is best observed in Figs. 13 and 14, where the test results can be compared with the corresponding theoretical curves for the same d_0/R values.

Table 1 summarizes the test results and theoretical predictions on the ultimate strength of columns. As can be seen a fairly good agreement between theory and experiment has been obtained in this investigation.

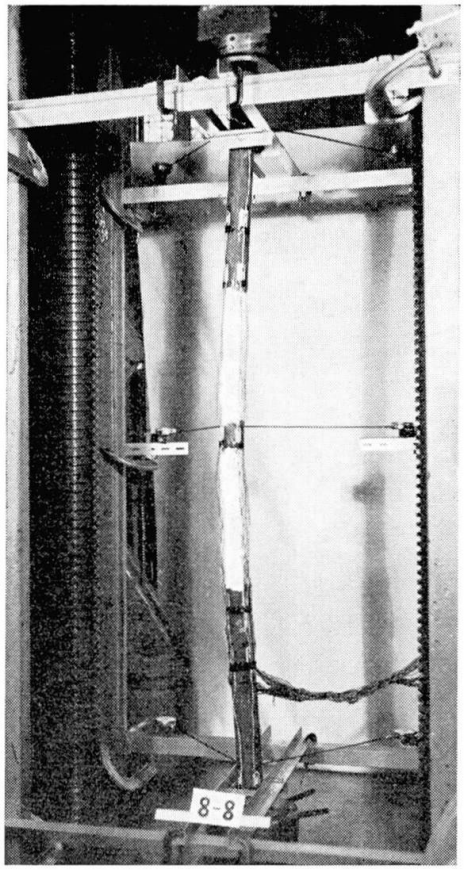

Fig. 16. Column test.

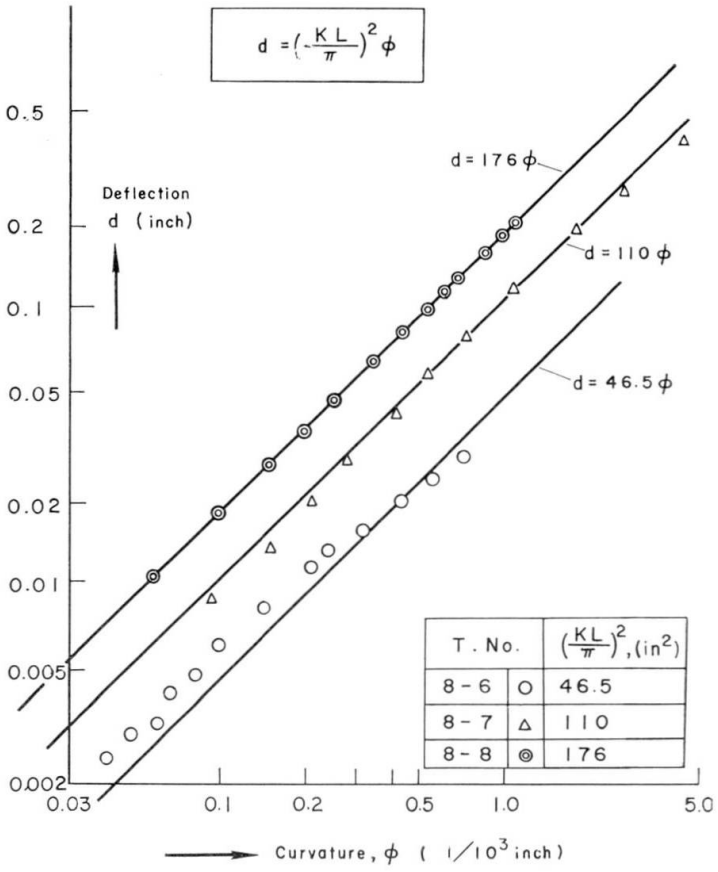

Fig. 17. Relationship between deflection and curvature.

Table 1. Comparison between theory and test results on the ultimate strength of columns

Test No.	Length L (in)	Generalized Slenderness Ratio, η	Initial Deflection d_0/R	Theory P_{max}/P_y	Test P_{max}/P_y
A 1—6	40	0.658	0.028	0.89	0.89
1—7	62	0.979	0.012	0.82	0.79
14—6	40	0.666	0.011	0.97	0.965
14—7	62	0.976	0.036	0,72	0.72
B 8—6	40	0.626	0.013	0.87	0.885
8—7	62	0.940	0.051	0.66	0.675
8—8	80	1.200	0.041	0.52	0.51

Group A: Air-cooled or stress-relieved specimens (low residual stresses)
Group B: Quenched specimens (high residual stress)

V. Summary and Conclusion

1. Using a temperature-dependent stress-strain relationship and Mises' yield criterion, the thermal transient and residual stresses in a heat-treated solid circular cylinder were analyzed. A step-by-step procedure for obtaining an approximate solution was presented. As an example, numerical calculations were performed for the case of a water-quenched steel bar.

Residual stress measurements on specimens, which were subjected to such heat treatments as quenching, air-cooling or stress-relieving, were made by using the "combined-method" together with the ordinary "boring-out method". For either tempering, air-cooling or stress-relieving the residual stresses were less than about 15—20% of the yield stress of the material, whereas the as-quenched specimens contained considerably higher compressive residual stresses (axial and tangential) in the outer part of the cross section. (Figs. 4 and 5.) A satisfactory correlation between the theoretical analysis and the test results has been obtained on the magnitude and distribution of the residual stresses in a water-quenched steel.

2. The influence of triaxial residual stresses in column members upon their compressive strength in the inelastic range was investigated by introducing the "equivalent residual stress" concept. Hence the problem was reduced to the case of uniaxial residual stress, thereby simplifying the analysis to a large extent. With a known pattern of the equivalent residual stress and the static yield stress of the material, the average stress-strain relationship for a short column was obtained and verified by stub column tests (Fig. 7).

A lower and an upper bound for the inelastic buckling load of round columns, the "true" tangent modulus load, and the reduced modulus load, were obtained in terms of the tangent modulus, E_t. It was then shown that the true tangent modulus load is proportional to $(E_t/E)^2$, whereas the reduced modulus load is approximately proportional to the ratio (E_t/E). (Eqs. (31) and (37).)

3. The maximum load-carrying capacity of axially loaded round columns was analyzed by including the effects of both thermal residual stresses and initial deflections. Members containing high residual stresses caused by water-quenching, for example, carry approximately a 10—20% lower load than air-cooled or stress-relieved steel columns, provided that their generalized slenderness ratio η and initial deflections d_0 are the same (Fig. 15). In general, the reduction of the ultimate strength due to initial deflection is quite pronounced, especially in the region $\eta = 1.0$.

To verify the theoretical analysis of the ultimate strength, column tests were performed. Fair agreement between the theoretical predictions and the experimental results was obtained (Table 1).

4. The methods used in this paper may be extended to the solution for hollow circular cylindrical columns if their wall thickness is sufficiently large

so that local buckling is eliminated. If the magnitude and the distribution of residual stresses in the outer part of the cross section are similar, then the results obtained for solid circular columns can be approximately used for the hollow cylindrical columns, because the yielding usually does not penetrate deeply into the cross section before the ultimate load is reached.

Acknowledgements

This work has been carried out at the Fritz Engineering Laboratory, Lehigh University, Bethlehem, Pennsylvania, as part of a research project on Circular Columns of USS "T-1" Constructional Alloy Steel sponsored by the United States Steel Corporation.

The authors wish to express their gratitude to Dr. Robert L. Ketter and Dr. Theodore V. Galambos for contributing fruitful discussions and suggestions.

Mr. Dian P. Jen assisted in the testing, in performing the numerical computations and in drawing the figures. His cooperation is gratefully acknowledged.

Nomenclature

Common Notations:

Subscript r = Radial component
Subscript θ = Tangential component
Subscript z = Axial component
Subscript i = $1, 2, 3, \ldots N$
Δ = Increment

Functions and Notations:

A	Cross sectional area
B_1, B_2 and B_3	Coefficients in differential equation, Eq. (7)
C_i^{i+1}, C_i^{i-1}, etc.	Ratios of modulus of elasticity, e. g. $C_i^{i+1} \equiv \frac{E(\rho_{i+1})}{E(\rho_i)}$, $C_i^{i-1} \equiv \frac{E(\rho_{i-1})}{E(\rho_i)}$, etc.
E	Young's modulus
$E(T)$	Temperature-dependent modulus of elasticity
E_t	Tangent modulus of stub column
I	Moment of inertia
I_e	Effective moment of inertia
J_0, J_1	Bessel function of order zero and one, respectively
J_2	Second invariant of deviatoric stress tensor, see Eq. (15)
$\bar{J}_2(\tau_1, \Delta)$	Function, see Eq. (17)

L	Length of column
M	Bending moment
N	Number of division
P	Axial thrust
P_{cr}	Critical load as defined by Eq. (28)
P_{max}	Maximum load
P_r	Reduced modulus load
P_t	Tangent modulus load
P_y	Full plastic load ($=\sigma_y A$)
Q_θ, Q_z	Incremental resultant force in tangential and axial direction, respectively, due to correction stress
R	Radius of cross section
T	Temperature
T_0	Initial temperature
$U(\lambda, \varphi)$	Axial thrust function $= P/P_y$
$V(\lambda, \varphi)$	Moment function $= \dfrac{M}{P_y R}$
a, b	Constants in equivalent residual stress pattern
c	Constant for cooling rate, see Eq. (1)
d	Deflection of effective column at mid-length
d_0	Initial deflection of effective column at mid-length
e	Proportionality factor $= \dfrac{[\Delta \sigma_{r,\theta,z}]_p}{\Delta \sigma_{r,\theta,z}}$
k	Effective column length factor
m_i	Real root of Eq. (2)
n	Constant in equivalent residual stress pattern
r	Coordinate (radial direction)
r_e	Radius of elastic core
r_0	Radius of gyration ($=R/2$)
s	Distance between centroidal axis and neutral axis
$\bar{s}$	Parameter $= s/R$
t	Time
$u(z)$	Lateral deflection of column
$v(r)$	Radial displacement
x	Coordinate (in the direction of lateral deflection)
z	Coordinate (axial direction)
$\alpha(T)$	Linear thermal expansion coefficient
ϵ	Strain (compressive strain is taken positive)
ϵ_{ave}	Average strain
η	"Generalized" slenderness ratio $= (k L/r_0)(1/\pi)\sqrt{E/\sigma_y}$
θ	Coordinate (tangential direction)
θ^*	Parameter for elastic-plastic boundary in the cross section
κ	Thermal diffusivity
λ	Parameter $= \sigma_0/\sigma_y$

μ	Parameter for elastic-plastic boundary in the cross section
ν	Poisson's ratio
ρ	Non-dimensionalized coordinate $= r/R$
ρ_e	Parameter for radius of elastic core $= (r_e/R)$
ρ_0, ρ_π	Parameters for elastic-plastic boundary in the cross section
σ	Stress (compression is taken positive)
σ_{ave}	Average stress
σ_e	Equivalent residual stress
σ_l	Linear stress
σ_0	Stress at the center of cross section as defined by Eq. (41)
$\bar{\sigma}$	Correction stress
σ_r	Transient or residual stress in radial direction
σ_θ	Transient or residual stress in tangential direction
σ_y	Yield stress in simple tension or compression
σ_z	Transient or residual stress in axial direction
$\Delta\sigma_z'$	Transient stress in axial direction when both ends are fixed (increment)
$[\Delta\sigma_{r,\theta,z}]_p$	Transient stress in plastic range (increment)
$\Delta\bar{\sigma}_{r,\theta,z}$	Correction of transient stress in plastic range (increment)
$\Delta\bar{\bar{\sigma}}_{r,\theta,z}$	Correction of transient stress in elastic range (increment)
τ	Non-dimensional parameter for time $= \kappa_t/R^2$
Φ	Curvature
φ	Non-dimensional parameter for curvature $= \frac{ER}{\sigma_y}\Phi$
ω	Incremental radial displacement (non-dimensionalized) $= \frac{\Delta v}{R}$

Appendix

Geometrical Illustration of the Assumption

$$\frac{[\Delta\sigma_r]_p}{\Delta\sigma_r} = \frac{[\Delta\sigma_\theta]_p}{\Delta\sigma_\theta} = \frac{[\Delta\sigma_z]_p}{\Delta\sigma_z} = e, \qquad (0 \leqq e \leqq 1)$$

in Art. II. 1. c:

The transient stress state at an arbitrary time τ can be illustrated in the three-dimensional coordinate system shown in Fig. 18. In this figure, point A denotes the stress state at $\tau=\tau_1$, and the vector $\overrightarrow{AC}$ represents the elastically computed stress increment from $\tau=\tau_1$ to $\tau=\tau_2\,(\Delta\tau=\tau_2-\tau_1)$, its components being $\Delta\sigma_r$, $\Delta\sigma_\theta$ and $\Delta\sigma_z$.

If yielding takes place during this interval $\Delta\tau$, the vector $\overrightarrow{AC}$ would extend beyond the yield surface S_2 defined by

$$J_2(\tau=\tau_2) = \tfrac{1}{3}\sigma_y^2(\tau=\tau_2)$$

(see Eq. 15). The actual incremental stress vector in the plastic zone, whose components are $[\Delta\sigma_r]_p$, $[\Delta\sigma_\theta]_p$ and $[\Delta\sigma_z]_p$ should terminate on the yield surface S_2 after intersecting the point B (which corresponds to the initiation of yielding). In general, the location of the terminal point B' depends upon the plastic flow that occurred during yielding. For a material with an idealized stress-strain relationship as assumed in Art. II. 1. b, there is no increase of stress in the case of a uniaxial stress state. Even when the stress condition is

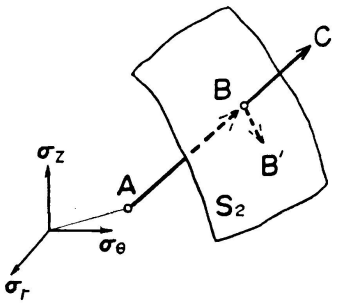

Fig. 18. Transient stress state.

triaxial, the change of the stress component during yielding (vector BB') will be small as compared with the increment up to the initiation of yielding (vector $\overrightarrow{AB}$). Therefore,

$$\overrightarrow{AB'} \cong \overrightarrow{AB} = e\,\overrightarrow{AC},$$

where e is a factor of proportionality. This relationship leads to the assumption

$$\frac{[\Delta\sigma_r]_p}{\Delta\sigma_r} = \frac{[\Delta\sigma_\theta]_p}{\Delta\sigma_\theta} = \frac{[\Delta\sigma_z]_p}{\Delta\sigma_z} = e.$$

If the time interval $\Delta\tau$ is sufficiently small, this assumption will be satisfactory.

References

1. Hetényi, M., Handbook of Experimental Stress Analysis, pp. 459—578, John Wiley and Sons, Inc., New York, 1950.
2. Weiner, J. H. and Huddleston, J. V., Transient and Residual Stresses in Heat-Treated Cylinders, Journals of Applied Mechanics, Vol. 26, Series E, No. 1, p. 31 (1959).
3. Osgood, W. R., The Effect of Residual Stresses on Column Strength, Proc. First National Congress of Applied Mechanics, p. 415 (June 1951).
4. Yang, C. H., Beedle, L. S. and Johnston, B. G., Residual Stress and the Yield Strength of Steel Beams, Welding Journal, Vol. 31, No. 4, p. 205-s (April 1952).
5. Huber, A. W. and Beedle, L. S., Residual Stress and the Compressive Strength of Steel, Welding Journal, Vol. 33, No. 12, p. 589-s (December 1954).
6. Thürlimann, B., Der Einfluß von Eigenspannungen auf das Knicken von Stahlstützen, Schweizer Archiv für angewandte Wissenschaft und Technik, Heft 12, 23 (1957).
7. Duberg, J. E. and Wilder, T. W. III, Inelastic Column Behavior, NACA Tech. Report, 1072, pp. 287—302 (1952).

8. FUJITA, Y., Built-up Column Strength, Fritz Laboratory Report No. 249.2, Lehigh University, August, 1956 (Ph. D. Dissertation).
9. GALAMBOS, T. V. and KETTER, R. L., Columns Under Combined Bending and Thrust, Journal of the Engineering Mechanics Division (Proceedings of the American Society of Civil Engineers), Vol. 85, No. EM2 (April 1959).
10. CARSLAW, H. S. and JAEGER, J. C., Conduction of Heat in Solids, p. 176, Oxford University Press, London, 1947.
11. TIMOSHENKO, S. and GOODIER, J. N., Theory of Elasticity, p. 408, 2nd ed., McGraw-Hill Book Company, Inc., New York, 1951.
12. WATANABE, M., SATO, K. and GODA, S., Thermal and Residual Stresses of Circular Cylinders Suddenly Cooled From the Uniformly Heated Condition, Journal of the Society of Naval Architects of Japan, Vol. 88, p. 155 (1955).
13. USS "T-1" Constructional Alloy Steel, United States Steel Corporation Publication No. ADUCO 01060-59.
14. NITTA, A., KETTER, R. L. and THÜRLIMANN, B., Strength of Round Columns of USS "T-1" Steel, Fritz Laboratory Report No. 272.1, Lehigh University (October, 1959).
15. SACHS, G., Der Nachweis innerer Spannungen in Stangen und Rohren, Zeitschrift für Metallkunde, Vol. 19, pp. 352—357 (1927).
16. BÜHLER, H., Complete Determination of the State of Residual Stress in Solid and Hollow Metal Cylinders, Residual Stresses in Metals and Metal Construction, edited by W. R. Osgood, pp. 305—329, Reinhold Publishing Corporation, New York, 1954.
17. TALL, L. and KETTER, R. L., On the Yield Properties of Structural Steel Shapes, Fritz Laboratory Report No. 220A.33, Lehigh University (November 1958).
18. BLEICH, F., Buckling Strength of Metal Structures, p. 8, McGraw-Hill Book Co., Inc., New York, 1952.
19. WILDER, T. W. III, BROOKS, W. A., Jr. and MATHAUSER, E. E., The Effect of Initial Curvature on the Strength of an Inelastic Column, NACA Tech. Note 2872 (January 1953).

Summary

This paper treats primarily problems on the formation of cooling residual stresses due to heat treatments and their effect on the load-carrying capacity of high yield-strength constructional alloy steel circular columns.

First, the thermal transient and residual stresses in a solid cylinder are studied on the basis of a temperature-dependent stress-strain relationship and Mises' yield criterion. An approximate solution computed by a step-by-step method is presented with a numerical example for the case of a water-quenched alloy steel. The result is checked with experimental measurements performed by the "combined method" together with the ordinary "boring-out method".

With proper information on the residual stresses thus obtained, an average stress-strain curve is readily furnished for bars with each heat treatment. Then a solution to the inelastic buckling strength of round columns is developed on the basis of (1) the tangent modulus concept and (2) the reduced modulus concept.

As a final objective, the ultimate strength of circular columns is analyzed taking into account the effects of the residual stresses and initial out-of-straightness of column members. It is shown that good correlation exists between the theoretical predictions and column test results.

Résumé

Les auteurs traitent principalement de problèmes portant sur la formation de contraintes résiduelles de refroidissement dues aux traitements à chaud, et de leur influence sur la charge de compression supportée par les barres circulaires en acier allié à haute limite élastique.

Tout d'abord, cette étude porte sur les contraintes thermiques transitoires et résiduelles dans un cylindre solide sur la base d'une relation contrainte — allongement dépendant de la température et du critère d'écoulement de Mises. Une solution approximative, évaluée par une méthode de proche en proche, est présentée, avec un exemple numérique, dans le cas d'un acier allié trempé à l'eau. Le résultat est contrôlé par des mesures expérimentales réalisées à l'aide de la «méthode combinée» utilisée de pair avec la «méthode de trépanation» ordinaire.

Les contraintes résiduelles étant ainsi connues, on peut établir facilement une courbe moyenne donnant la relation contrainte — allongement des barres, pour chaque traitement à chaud. Puis, une solution donnant la résistance au flambage des barres circulaires dans le domaine plastique est développée sur la base de la théorie du «module tangent» et de celle du «module réduit».

Comme objectif final, la résistance limite est analysée en tenant compte des effets des contraintes résiduelles et des imperfections initiales des barres. On montre qu'il existe une bonne corrélation entre les prédictions théoriques et les résultats des essais faits sur les barres.

Zusammenfassung

Die Arbeit befaßt sich mit der Ausbildung von Eigenspannungen infolge Wärmebehandlung und deren Einfluß auf die Tragfähigkeit von Säulen mit Kreisquerschnitt aus hochwertigem Baustahl.

Zuerst werden die instationären Wärmespannungen und die sich nach Abkühlung ergebenden Eigenspannungen in einem Kreiszylinder auf Grund eines temperaturabhängigen Spannungs-Dehnungs-Gesetzes und der Misesschen Fließbedingung untersucht. Eine schrittweise Näherungslösung mit einem numerischen Beispiel für den Fall eines mit Wasser abgeschreckten Zylinders aus legiertem Stahl wird hergeleitet. Das Ergebnis wird mit Meßresultaten verglichen, welche an Probestücken durch eine «Kombinations-

Methode», zusammen mit der gebräuchlichen «Ausbohrungs-Methode», erhalten wurden.

Aus der Kenntnis des Eigenspannungszustandes lassen sich durchschnittliche Spannungs-Stauchungs-Kurven für Stützen herleiten, die unterschiedliche thermische Behandlungen erfahren haben. Daraus wird die Knickfestigkeit von Säulen mit Kreisquerschnitt entwickelt, und zwar sowohl nach der «Tangenten-Modul-Theorie» als auch nach der «Reduzierten-Modul-Theorie».

Schließlich wird noch die Tragfähigkeit der Säulen unter Berücksichtigung der Eigenspannungen und anfänglichen Ausbiegungen untersucht. Ein Vergleich zeigt eine gute Übereinstimmung der berechneten Werte mit Versuchsresultaten.